

NATIONAL RADIO ASTRONOMY OBSERVATORY  
GREEN BANK, WEST VIRGINIA

ELECTRONICS DIVISION INTERNAL REPORT No. 152

FIRST TESTS OF AN ANTENNA MEASURING INSTRUMENT  
ON THE 36-FOOT TELESCOPE

J. M. PAYNE, J. M. HOLLIS, AND J. W. FINDLAY

DECEMBER 1974

NUMBER OF COPIES: 150



FIRST TESTS OF AN ANTENNA MEASURING INSTRUMENT  
ON THE 36-FOOT TELESCOPE

---

J. M. Payne, J. M. Hollis, and J. W. Findlay

TABLE OF CONTENTS

	<u>Page</u>
1.0 <u>Introduction</u> .....	1
2.0 <u>Principle of Operation</u> .....	2
3.0 <u>Description of Equipment</u> .....	4
3.1 The Curvature Measuring Instrument .....	4
3.2 The Towing Mechanism .....	4
3.3 The Computer Interface .....	5
4.0 <u>The On-Line Data Taking Reduction</u> .....	5
4.1 Theoretical Data .....	5
4.2 Taking Data .....	7
5.0 <u>The Measurements</u> .....	8
6.0 <u>The Results</u> .....	11
6.1 Data Handling .....	11
6.2 The Measurement Accuracy (M) .....	12
6.3 The Telescope Surface .....	12
7.0 <u>Conclusions and Further Work</u> .....	13

LIST OF FIGURES

1	The Principle of the Method .....	2
2	The Measurement of K .....	3
3	The Curvature Measuring Instrument .....	15
4 (a), (b)	Raw Data for Two Successive Runs Over the Same Radius .....	16
4 (c)	The Difference between (a) and (b) .....	17
5	The 3000-4000 Count Section of Figure 4(b) with Expanded Scales .....	18
6 (a)	The Result of the First Integration showing the Change of $\theta$ as S Changes .....	19
6 (b)	The Second Integration showing the Change of Y with S .....	20
7	The Difference between the Y Curves for Two Successive Runs Over the Same Radius of the Dish .....	21
8 (a), (b)	Maps of the Departures of the Reflector Surface from the Best-Fit Paraboloid. (a) and (b) are derived from separate sets of measurements. ....	22



## 1.0 Introduction

Over the past few years we have investigated various methods of measuring high precision antennas. Our previous approach to the problem has been confined to investigating methods of measuring distance as accurately as possible. The antenna surface may then be surveyed by measuring distance between many points on the surface and one or two reference points. For measuring a millimeter wave antenna the accuracy required of these range measurements is generally better than 0.1 mm at ranges up to about 60 m, the exact value depending on the size of the antenna and the intended frequency of operation.

Two methods have evolved from this work. The first (1) uses a microwave method to measure distances from the focal point of the antenna to transponders on the parabolic surface. This is a useful technique for measuring the deformations of the surface that may result from movement of the antenna or changes in ambient temperature. However, for various reasons this method is not well suited to the measurement of absolute distance so necessary for the initial setting of the antenna.

The second method (2) uses a modulated laser beam to measure distance from both the vertex and the focus of the antenna to optical corner cubes on the surface. The required accuracy of the range measurement is achievable and this method is certainly feasible. Obvious disadvantages are the need for many corner cube reflectors, a system for steering the laser beam to different reflectors, and an efficient data collecting system.

The method described in this report uses a completely different principle. Essentially the curvature of the surface is measured with a high accuracy at many points along a radius of the surface. These curvature values are then integrated twice with respect to the distance along the surface by an on-line computer, the result being the  $Y$  coordinate of the surface as a function of the

distance along the surface. This is repeated for different radii and a contour map of the surface generated.

A trial set of measurements recently made on the 11-meter antenna in Tucson indicates that the method gives an accuracy close to that required for the measurement of a millimeter wave antenna. The method has the advantages of being quick, simple, and inexpensive (provided an on-line computer is available).

## 2.0 Principle of Operation

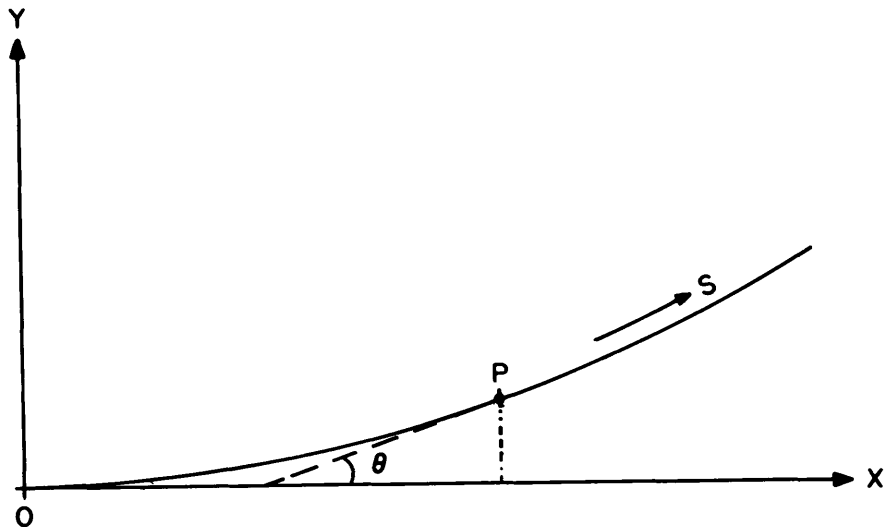


Figure 1 - The principle of the method.

Take any reasonable curve  $Y = f(X)$  as shown in Figure 1. At any point, P, the curvature, K, is given by:

$$K = \frac{d\theta}{dS} \quad (1)$$

where  $\theta$  is the slope of the curve and S is the distance measured along the curve from the origin.

The K value at any point on the surface may be measured by an accurately-constructed three-wheeled trolley with an electronic depth gauge mounted at its

mid-point as illustrated in a simplified form in Figure 2:

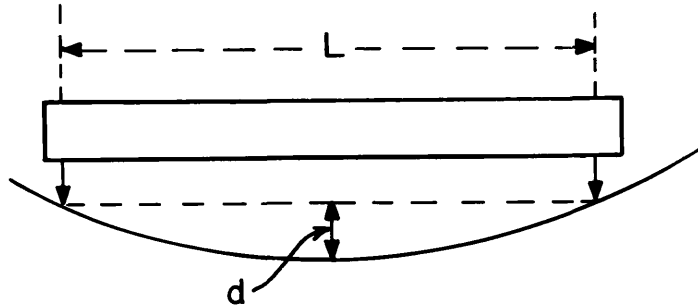


Figure 2 - The measurement of K.

L is the distance apart of the contact points of the wheels on the surface and d is the distance to the surface from the plane of the wheels at the mid-point of L. Then,

$$K = \frac{8d}{L^2 + 4d^2} \quad (2)$$

The distance S along the surface from the origin is measured by an incremental encoder attached to the front single wheel, giving 250 pulses per revolution. Each pulse corresponds to a change in S of about 0.6 mm. Pulses are numbered from 0, at the origin, to n. We start from the origin and move out along a dish radius. At each interval as indicated by the wheel transducer we record both  $K_n$  and  $S_n$  and compute  $\theta_n$  from (1):

$$\theta_n = \int_0^n K_n dS \quad (3)$$

At any point, P, we compute  $Y_n$  from

$$Y_n = \int_0^n \sin \theta_n dS \quad (4)$$

since

$$\sin \theta_n = \left( \frac{dY}{dS} \right)_n$$

The result of the two integrations therefore gives Y as a function of S. This may then be compared with the result expected from the perfect dish surface and contours of error may be displayed. We return later to the determination of the initial conditions which are needed to evaluate the integrals (3) and (4).

### 3.0 Description of Equipment

#### 3.1 The Curvature Measuring Instrument

A drawing of the curvature measuring instrument is shown in Figure 3. It is a three-wheeled trolley with the displacement transducer mounted half way between the two wheel axles. The wheels are 5.08 cm in diameter, and the distance between them is 50.00 cm. A microscope, used for aligning the trolley with the starting point is mounted 10.160 cm from the rear wheel axle. The tolerances on all dimensions are less than  $\pm 0.04$  mm.

The success of this type of measurement is very dependent on the accuracy of the displacement transducer. We used a transducer manufactured by Shaevitz Engineering that has a repeatability of  $10^{-4}$  mm and a linearity of about 0.01% over a range of  $\pm 0.5$  mm.

The wheel transducer used is an incremental encoder giving 250 pulses per wheel revolution. This corresponds to a pulse every 0.6384 mm of carriage movement.



### 3.2 The Towing Mechanism

Initially we had doubts about the feasibility of towing a carriage across the surface of the dish in a sufficiently repeatable manner. We decided to try the simplest approach first and then proceed to more exotic methods if necessary. The method used was to clamp an accurately made pulley assembly to the edge of the dish, carefully aligning a scribed line in the center of the pulley housing with a previously scribed line on the dish surface. A fine steel cable connected to the front of the trolley passed over this pulley and back to a small electric winch mounted at the center of the dish. The starting point was established by manually aligning the trolley, using the microscope, over a starting point marked on the surface. First tests showed that the trolley returned to its starting point with a surprising repeatability after being towed to the edge of the dish. In view of this, it was decided to use this very simple method for the first set of measurements.

### 3.3 The Computer Interface

The analog signal from the displacement transducer was interfaced to the PDP/11 telescope computer via a 15-bit A/D converter arranged so that the output from the converter was read by the computer at every wheel pulse transition.

The scaling was such that the least significant bit of the A/D converter represented a  $6.17 \times 10^{-5}$  mm movement of the displacement transducer.

## 4.0 The On-Line Data Taking and Reduction

### 4.1 Theoretical Data

The 11 meter telescope has a diameter of 10.97 m and a focal length of 8.778 m, giving X and Y surface dimensions related by

$$X^2 = 35.113 Y$$

Before the measurements were made on the antenna, a Fortran program was written to calculate the various values that could be expected from a measurement on a perfect 11 meter surface. The following relationships were used in the computation:

$$\Delta Y = \frac{\Delta S}{\sqrt{1 + C/4Y}} \quad (5)$$

$$K = \frac{2}{C[1 + 4Y/C]^{3/2}} \quad (6)$$

At every 100  $\Delta S$  increments the values of the various parameters were printed out. The computation shows that more than 8700 increments of  $\Delta S$  are needed to measure a complete radius; the curvature values do not change greatly across the surface and the tangential angle at the lip of the dish is approximately 17°. The distance  $d$  is 1.78 mm at the center of the dish and 1.58 mm at the edge.

#### 4.2 Taking Data

The center part of the dish was obstructed by the mounting brackets for the antenna electronics so that the starting point for each radial track was about 75 cm from the dish center. Thus, about 6200 values of  $K$  were recorded for each radial track.

Each data sample was stored on disk and at the end of the measurement the raw data was displayed on the CRT terminal.

The next step was to evaluate the curvature,  $K$ , from

$$K_n = \frac{8(d_n + D)}{L^2 + 4(d_n + D)^2} \quad (7)$$

where

$d_n$  = transducer reading at the  $n^{\text{th}}$  readout.

$D$  = transducer reading on flat surface.

As  $(d_n + D)$  changes only from 1.78 mm to 1.58 mm across the surface, we may absorb the very nearly constant  $4(d_n + D)^2$  into  $L^2$ .

The first integral to be computed is the value of  $\theta_n$

$$\theta_n = \int_0^n K_n dS + \theta_0 \quad (8)$$

which is the summation

$$\theta_n = \Delta S \sum_0^n K_n + \theta_0 \quad (9)$$

where  $\theta_0$  is the angle at the starting point. The starting point was well defined by theodolite measurements and we assumed the equation for the surface to be true from the origin to the measurement start point. Thus, the starting values of  $K$  and  $\theta$  were also well defined.

The  $Y$  coordinate at any point on the radius is given by

$$Y_n = \int_0^n \sin \theta \cdot dS + Y_0 \quad (10)$$

where  $Y_0$  is the starting value of  $Y$ .

This may be evaluated by the summation:

$$Y_n = \Delta S \sum_0^n \sin \theta_n + Y_0 \quad (11)$$

giving  $Y_n$  as a function of  $S$ .

After this integration the Y values along with the corresponding S values were stored on the disc. When all the radii have been computed the data was transferred to tape to enable a contour map to be produced on a larger machine equipped with a Calcomp plotter.

## 5.0 The Measurements

The 11-meter telescope has a 71.6 cm diameter hole in the center of the reflector surface, so it was necessary to establish an accurately known starting circle on the surface of the dish concentric with the hole. This was done using a theodolite mounted at the center of the dish and adjusted so that its vertical axis of rotation coincided with the telescope axis. Such an adjustment is a standard procedure in surveying radio telescopes and will not be described here.

We then set the theodolite to a suitable elevation angle and, using a short focal length eyepiece, scribed starting points around the starting circle on the surface every  $15^\circ$  in azimuth angle. The exact azimuth and elevation angles were noted and later used to calculate the starting point for each radius. The theodolite was then adjusted in elevation angle to align with the lip of the dish, and the finishing points for each radius were marked on the edge of the dish. The measurements were made along 23 such radii (one was unusable due to a bolt in the surface).

We believe our starting points to be accurate to within  $\pm 1$  mm. Careful measurements with a theodolite and a vertical machinist's rule convinced us that the center region of the dish was not seriously distorted, and our assumptions regarding the Y starting values were certainly valid to within  $\pm 0.05$  mm.

The surface measurements on the antenna were made on July 1, 1974 and took about 10 hours.

The antenna was positioned at the zenith and two people operated the measuring instrument. The data taking was controlled from the control room via a radio link\*, the results of each measurement being monitored on a CRT terminal.

The measurement sequence was simple. The trolley was positioned over the starting point using the microscope, the computer set to take data and the winch set in motion. After 6200 data points were taken the computer stopped, sounded an alarm, and the trolley was halted. The raw data was then examined on the CRT terminal to ensure the data looked reasonable. Each radius was measured twice with a time interval of perhaps 5-10 minutes between the runs. Two sets of data for the same radius are shown in Figure 7. The computer allowed the immediate subtraction of two runs for each radius; a typical result is shown in Figure 4.

The data takes approximately the form one would expect: the vertical transducer showing a decrease of approximately 0.2 mm over a radius. We were surprised to see in many of our results some repetitive features with two distinct characteristic lengths, one about an inch, the other several inches. We suspect this to be due to the machining process used to manufacture the antenna. Figure 5 shows a radius of the dish where this was particularly noticeable.

The point by point difference plots between successive scans over the same radius show small errors at the beginning with increasing errors towards the edge of the dish. The maximum errors were 0.03 mm peak to peak. The reason for the increase of error may be the wheel transducer occasionally giving out double transpositions, due perhaps to bounce in the towing cable. This error slowly accumulates. This is a fairly simple matter to correct. On some subtractions we noticed

---

\* We are indebted to Mr. C. Sparks for maintaining good R/T procedures over this link for a long and tiring day.

slight repetitive features of the correct period to be due to wheel eccentricity. These effects will be given attention in our future work.

Figure 6 shows the results of the first and second integrations for a single radial run. Figure 6(a) shows  $\theta$  to increase almost linearly with S and Figure 6(b) shows the almost parabolic variation of Y with S.

Figure 7 shows the results of subtracting the second integrations of two sets of data taken on the same radius about 10 minutes apart in time. This difference curve gives an idea of the repeatability of the method. It may be seen that the difference curve still resembles a parabola, the difference at the edge being 0.1 mm. This difference is almost certainly due to temperature effects slowly changing the focal length of the dish.\*

The antenna was damaged some years ago when the feed legs fell. There are thus some parts of the surface where our measurement system had insufficient range to measure accurately. We have not excluded these out-of-range readings from our analysis. The final maps will thus be somewhat in error and our measurement accuracy estimate may be slightly high. We measured each of the 23 radii twice so that at the end of the measurements we had sufficient data to generate two independent contour maps of the surface and to give a good estimate of the measurement accuracy.

## 6.0 The Results

### 6.1 Data Handling

At the end of the measurements two sets of (Y, S) data were available, each consisting of 21 values of Y for each of the 23 radii over which runs were made.

---

\* The measurements occupied most of a summer's day. The ambient temperature rose fairly uniformly for 6 hours at about 1°C per hour, and then remained fairly steady for 3 hours.

These two data sets were then further reduced and plotted as follows:

For each radius at a given azimuth the (Y, S) values were transformed to (Y, X) values. The S to X conversion was made using the relationship which would be true for a perfect paraboloid. This step does not introduce any serious errors in X and made the subsequent data handling possible by existing programs.

The X, Y, Z coordinates for each point were generated from the known X's and the azimuth angles of the radii.

A parabolic surface which best fitted the 483 measured points was then determined.\* This program found the best-fit when the following paraboloid parameters were varied: focal length, vertex displacement in the two orthogonal directions, vector direction of the paraboloid axis. The program then gave the departures of each of the 483 points from the best-fit surface and the RMS value for these departures.

Finally a standard Calcomp mapping program was used to give the two maps (Figure 8(a), (b)) of the departures from the best fit paraboloid of the measurements in the two sets of data.

## 6.2 The Measurement Accuracy (M)

The main reason for this first set of measurements was to find an estimate of the accuracy of the system when used on a telescope. This we did in the following way:

Let  $(Y_{1i})$  and  $(Y_{2i})$  be the Y values derived for the  $i^{\text{th}}$  point (of the 483 points measured) in the first and second sets of measurements, respectively.

$(Y_{1i})$  and  $(Y_{2i})$  will differ due to several causes; their difference should be a good measure of the accuracy of the system, and so we computed a value of M from:

---

\* We are indebted to Lee King for his program and help in carrying out this step.

$$M^2 = \frac{1}{N} \sum_N \left\{ \left( Y_1 \right)_i - \left( Y_2 \right)_i \right\}^2$$

where N = 483, the number of points.

We found M = 0.05 mm.

### 6.3 The Telescope Surface

The measurements were not designed to give a properly-sampled set of surface measurements, and a study of Figure 8 shows this to be true. The more heavily distorted areas of the surface are clearly under-sampled, but the mapping program shows this by placing the steep gradients mid-way between the measured radii. (The crosses on Figure 8 show the locations of the 483 points entered into the mapping program.)

The experiment should not, therefore, be taken to be a good overall map of the telescope, but it is interesting to give some results to show roughly what the telescope surface is like.

The RMS departures of the measured points from the best-fit paraboloid (giving equal weight to each point) are:\*

RMS in Set #1 = 0.453 mm

RMS in Set #2 = 0.456 mm

The focal lengths of the best-fit paraboloids are:

f in Set #1 = 8.7766 m

f in Set #2 = 8.7776 m

The nominal value is 8.7783 m.

---

\* The departures were also recalculated after weighting them to correspond to a 10 dB illumination taper and this resulted in an RMS for the telescope of 0.2 mm. This is in reasonable agreement with the value derived from the measured aperture efficiency at 3.5 mm wavelength.



## 7.0 Conclusions and Further Work

We are encouraged by the value of our estimate of measurement accuracy of 0.05 mm. This is not yet good enough if a system is needed for a dish of 25 m diameter working at 1.2 mm, yet the method is easy and rapid to use and the data taking and reduction is simple and automatic. The following points can be noted as a guide to work to improve the accuracy.

The lack of access to the dish center caused difficulty in making certain of our start conditions. It would have been desirable to start the curvature measures with the sensor each time over the dish center and with the cart wheels on a well-known flat (or curved) surface.

Our choice of wheel-bearings (which were roller-bearings of normal grade) might be improved.

The cart did not follow the desired radius with absolute accuracy. Some of our measuring error may be due to the divergence of the two (supposedly identical) tracks followed.

Our method of data reduction by forming the two integrations gives average values for the contours. As S. von Hoerner has pointed out, it would be possible to include each depth transducer reading into a more complex way of data reduction; one which could reproduce the profile to any degree of detail down to the limit set by  $\Delta S$ .

We plan to repeat the measurements on the 36-ft telescope; these will be done in such a way as to sample the surface more effectively. It may be that some improvements to the telescope by using a specially shaped subreflector (3) could be made.

References:

- (1) John W. Findlay and John M. Payne, "An Instrument for Measuring Deformations in Large Structures," IEEE Trans. Instr. Meas., Vol. IM-23, pp. 221-226, September 1974.
- (2) John M. Payne, "An Optical Distance Measuring Instrument," Rev. Sci. Inst., Vol. 44, pp. 304-306, March 1973.
- (3) E. A. Parker and P. R. Cowles, "Technique for Compensating for Reflector-Antenna-Surface Errors with Long Correlation Lengths," Electronic Letters, Vol. 8, pp. 366-7, July 1972.

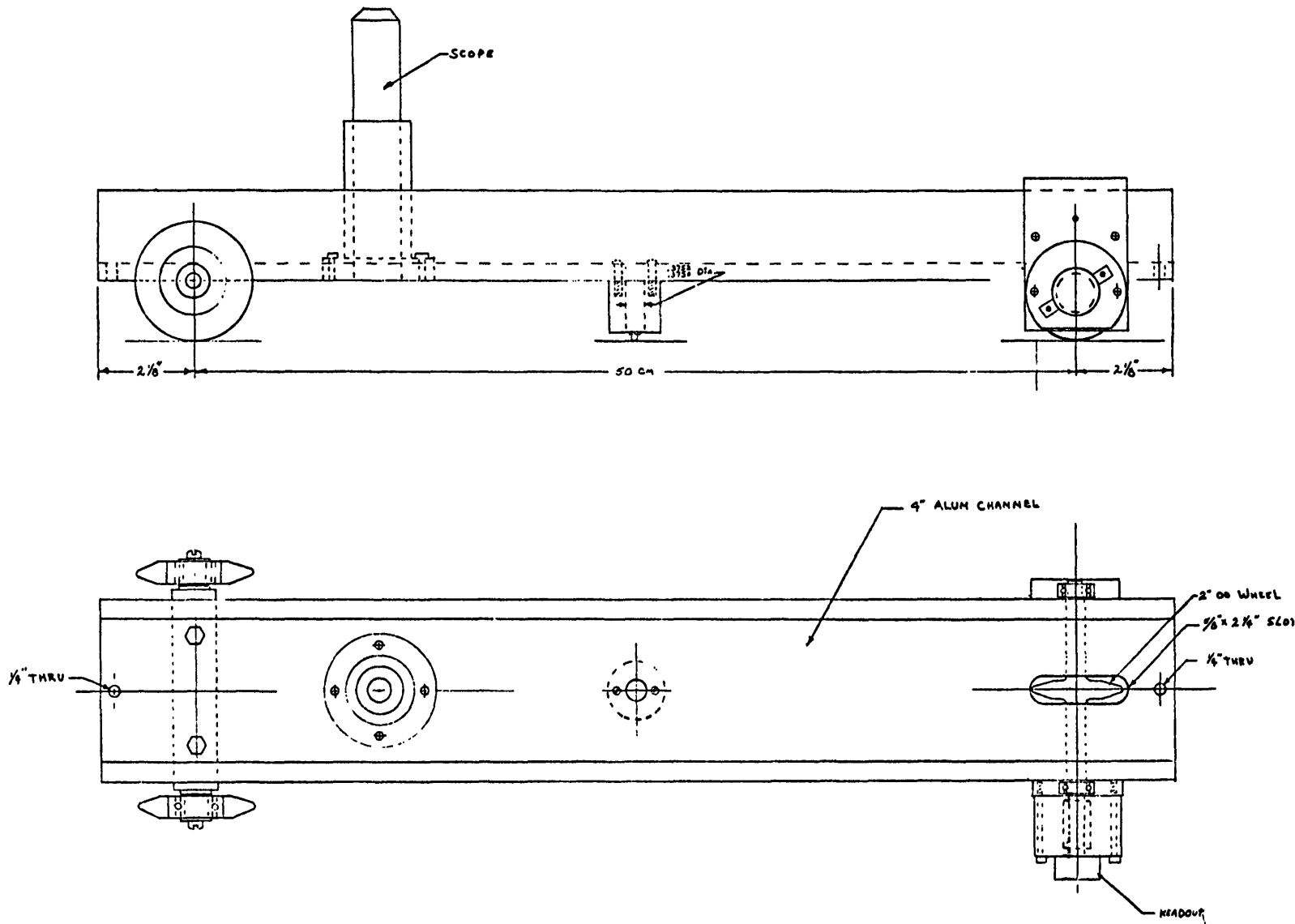


Figure 3 - The curvature measuring instrument

FINDLAYS SURFACE INSTRUMENT  
 FULL SCALE JAN 7, 1974

Figure 4 - (a), (b) - Raw data on two successive runs over the same radians.  
(c) - The difference between runs (a) and (b).

Vertical scale : 1 count =  $6.17 \times 10^{-5}$  mm  
Horizontal scale: 1 count = 0.6384 mm

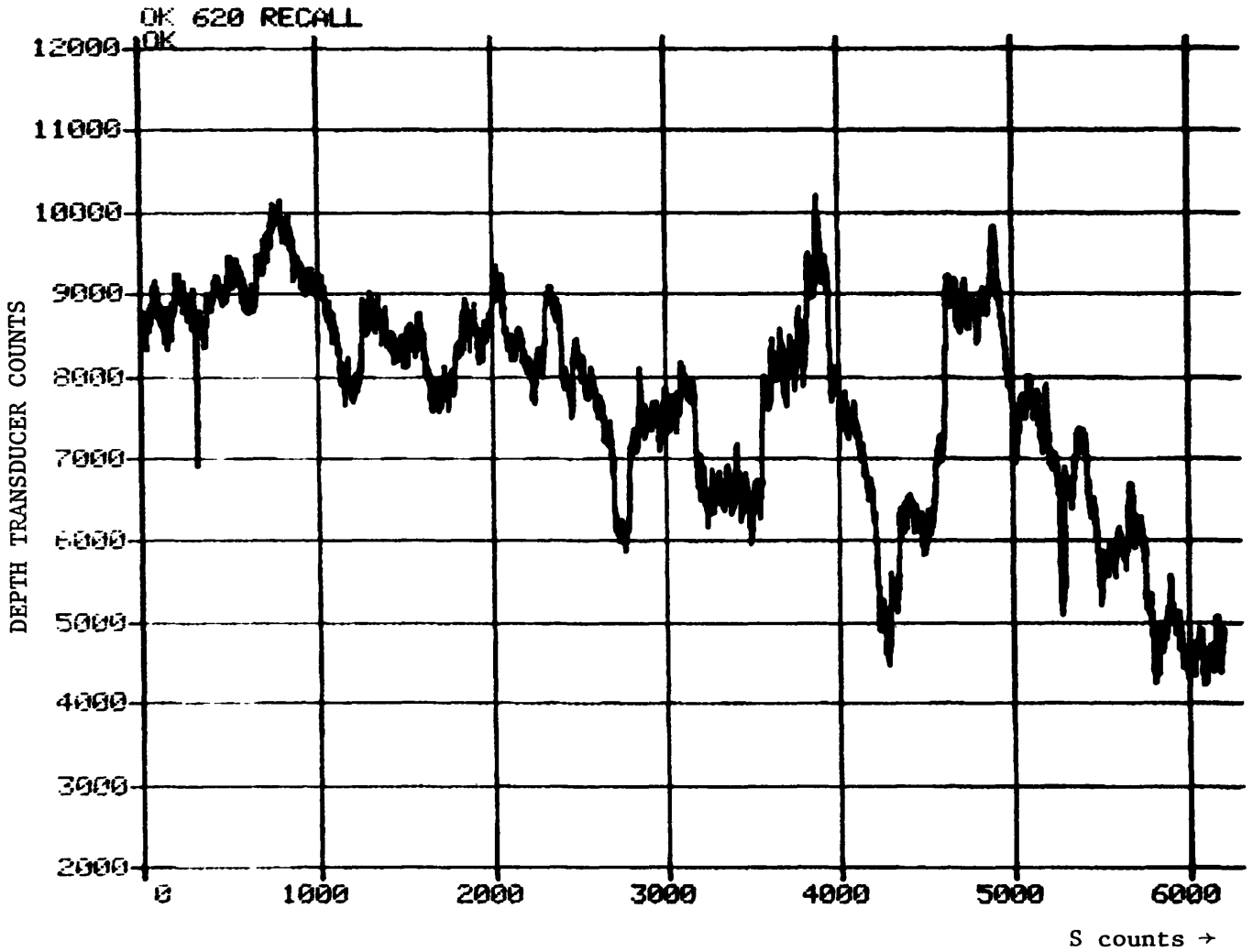


Figure 4(a)

Figure 4 - (a), (b) - Raw data on two successive runs over the same radians.  
(c) - The difference between runs (a) and (b).

Vertical scale : 1 count =  $6.17 \times 10^{-5}$  mm  
Horizontal scale: 1 count = 0.6384 mm

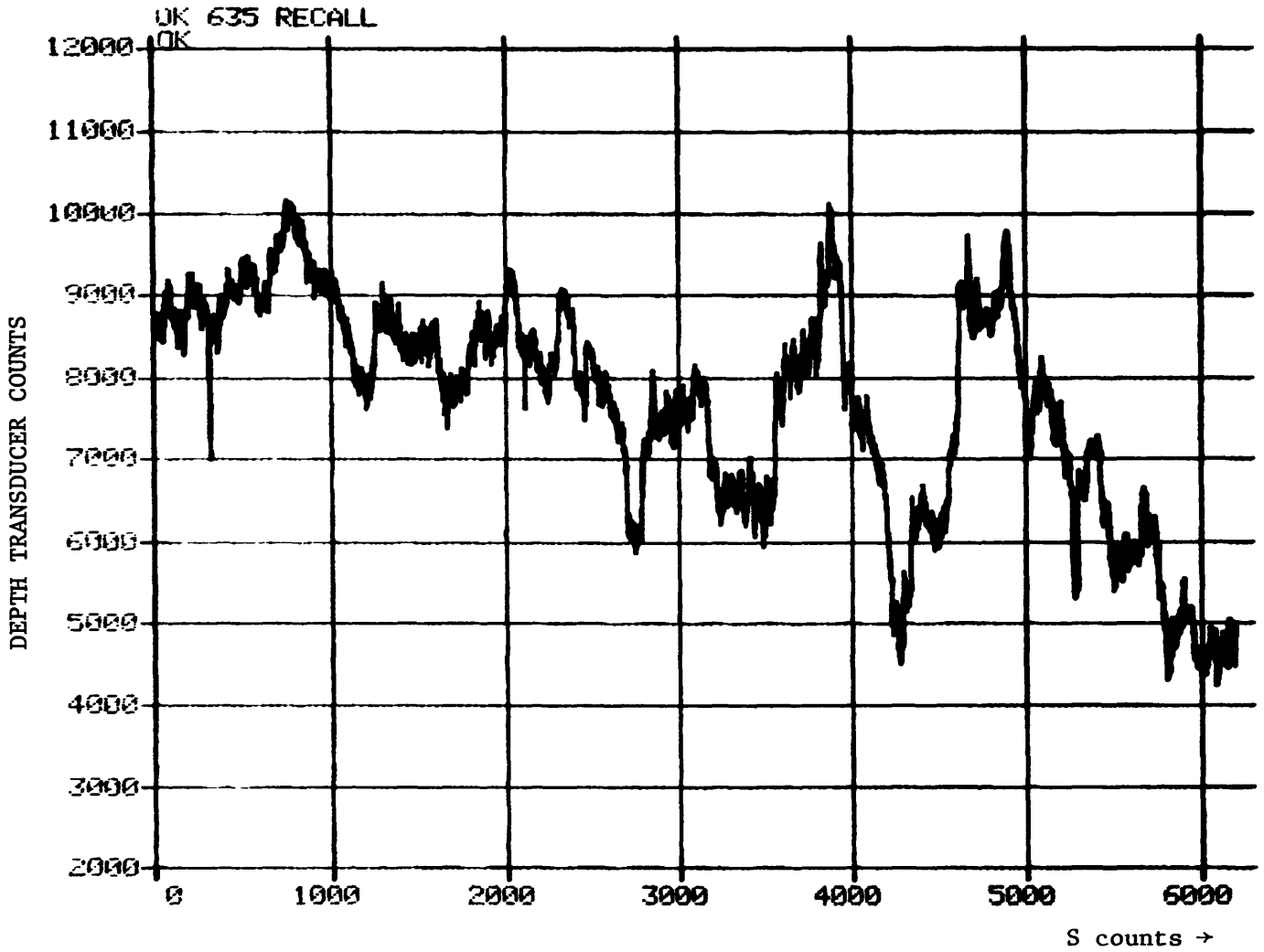


Figure 4(b)

Figure 4 - (a), (b) - Raw data on two successive runs over the same radians.  
(c) - The difference between runs (a) and (b).

Vertical scale : 1 count =  $6.17 \times 10^{-5}$  mm

Horizontal scale: 1 count = 0.6384 mm

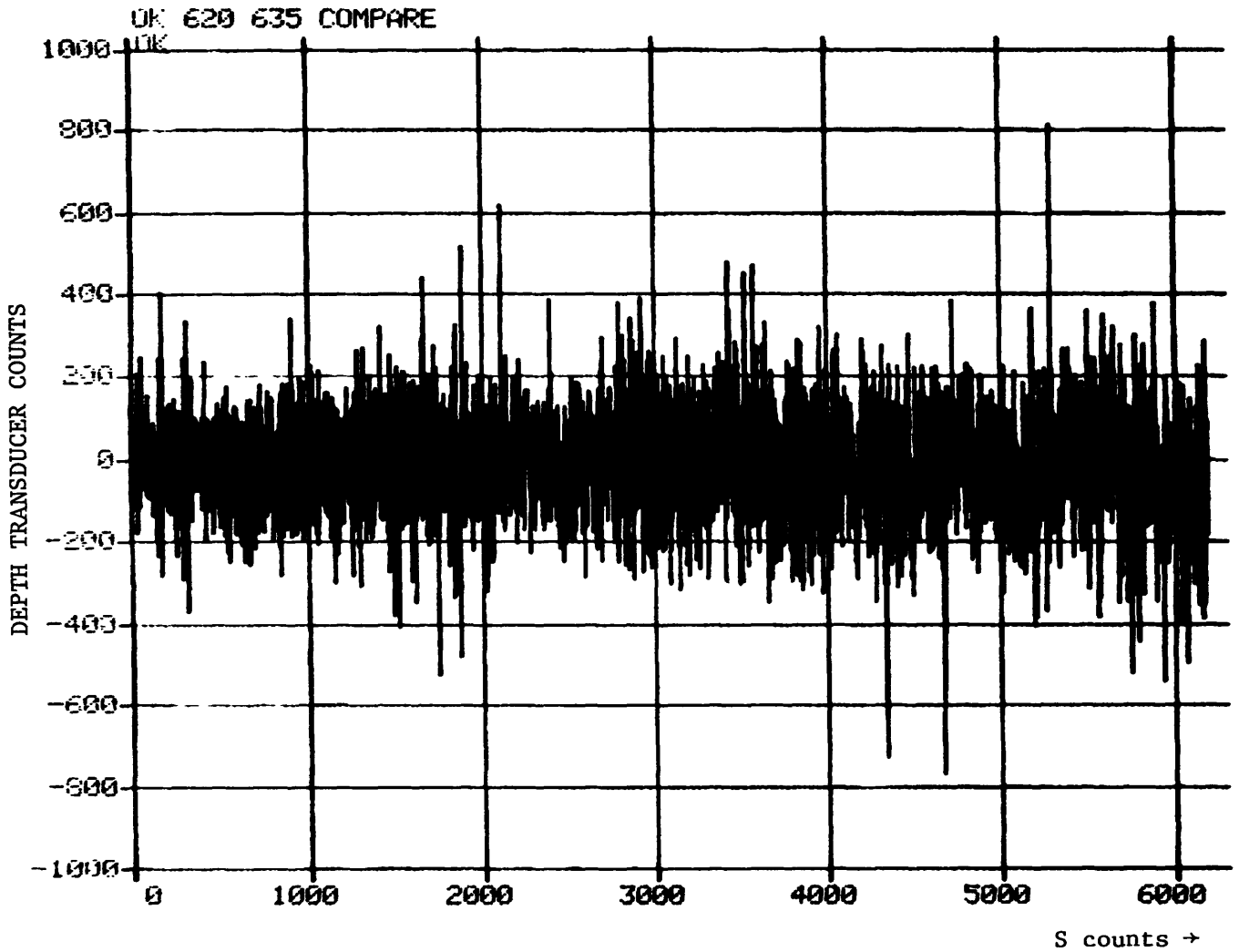


Figure 4(c)

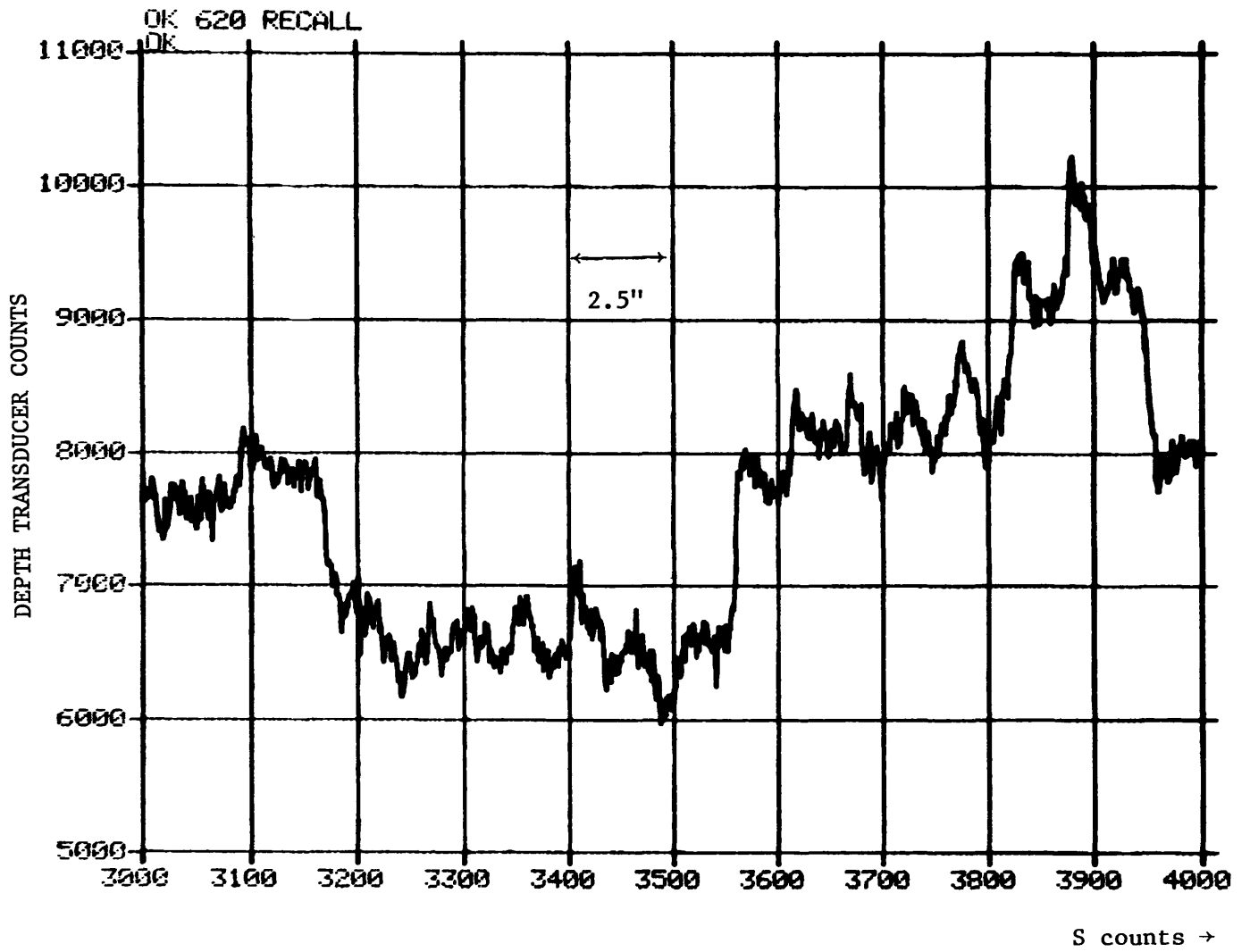


Figure 5 — The 3000-4000 count section of Figure 4(b) with expanded scales.

Figure 6 - (a) - The result of the first integration, showing the change in  $\theta$  and S changes.

(b) - The second integration, showing the change in Y with S.

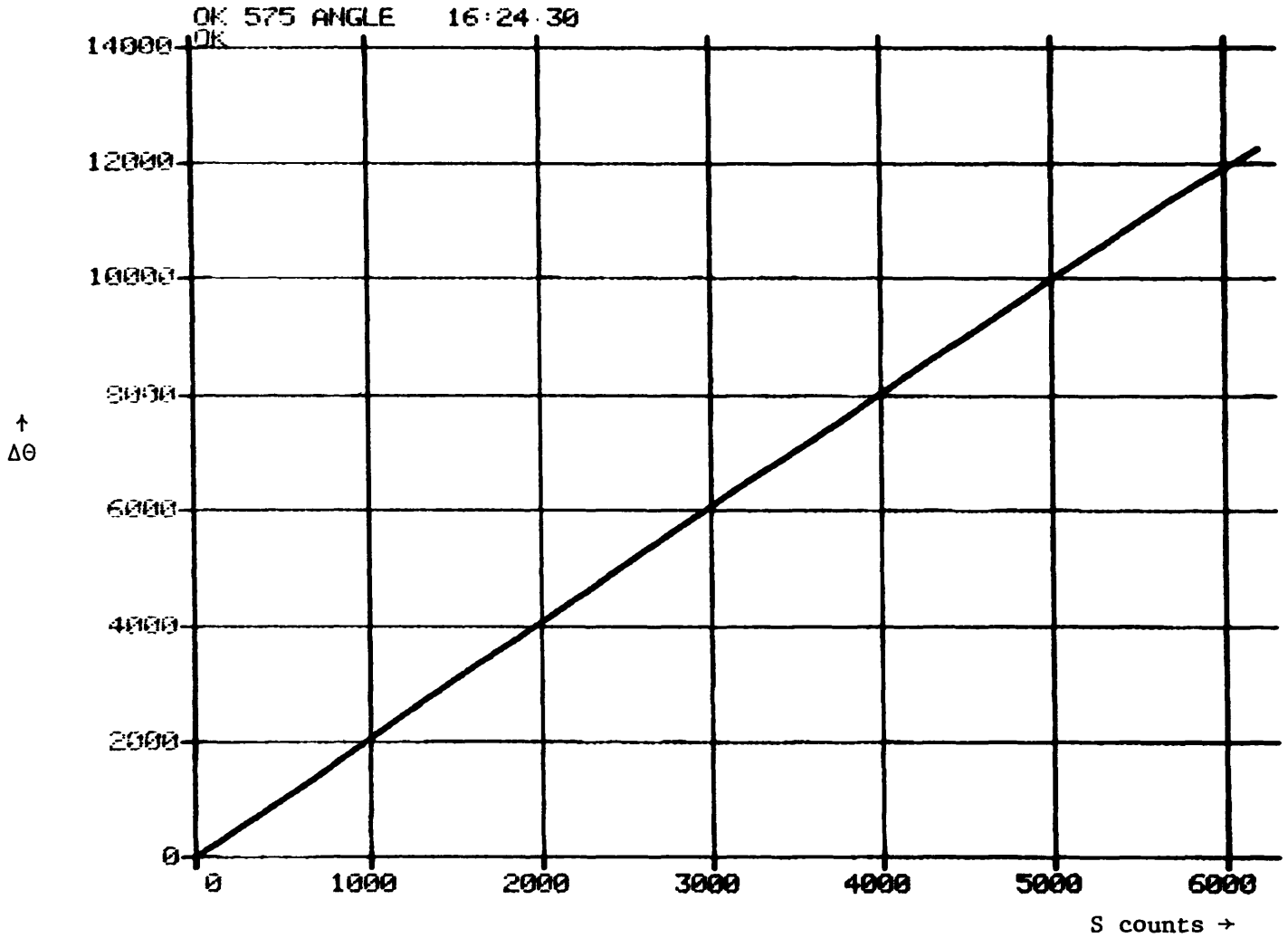


Figure 6(a)



Figure 6 - (a) - The result of the first integration, showing the change in  $\theta$  and S changes.

(b) - The second integration, showing the change in Y with S.

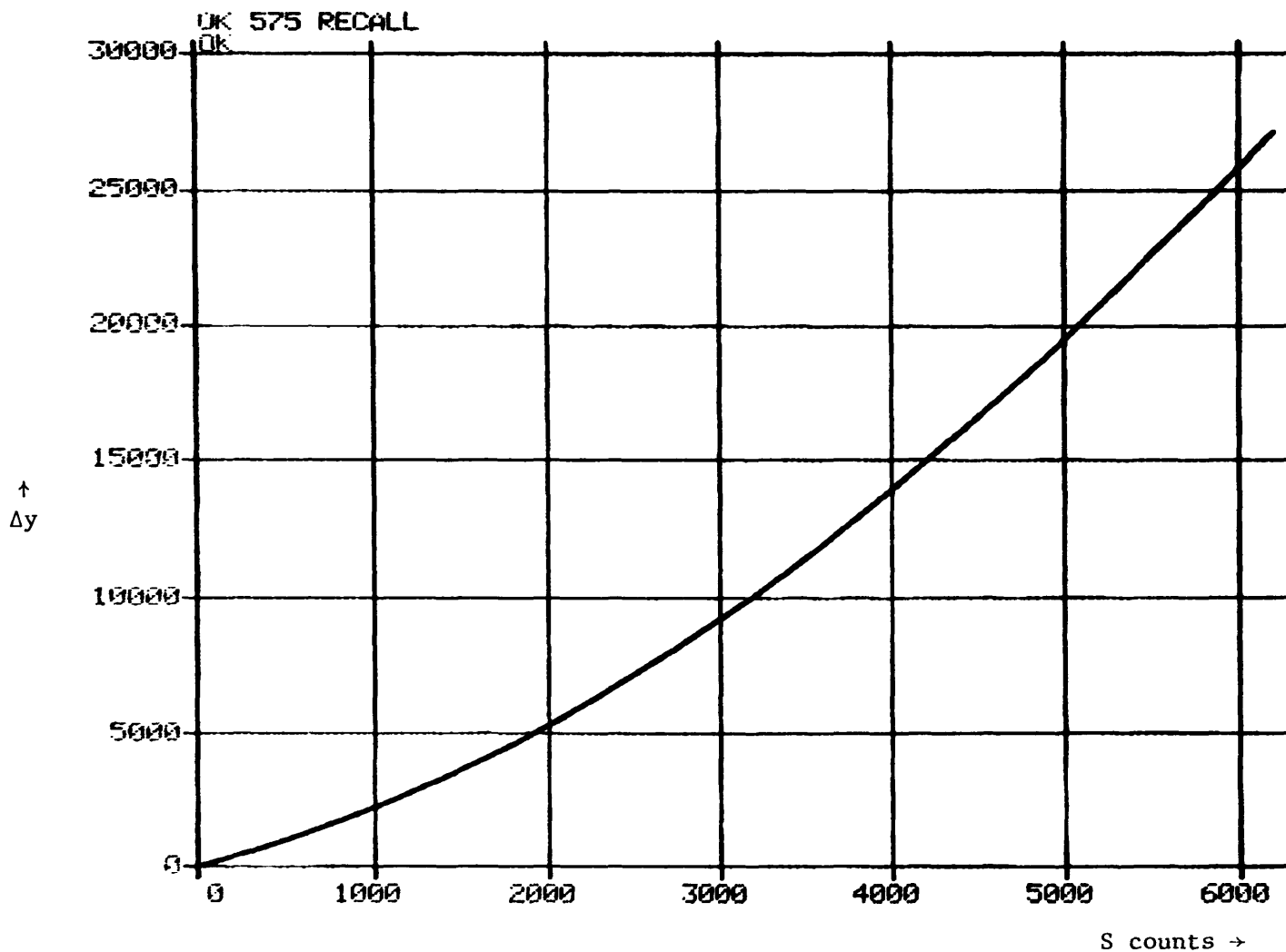


Figure 6(b)

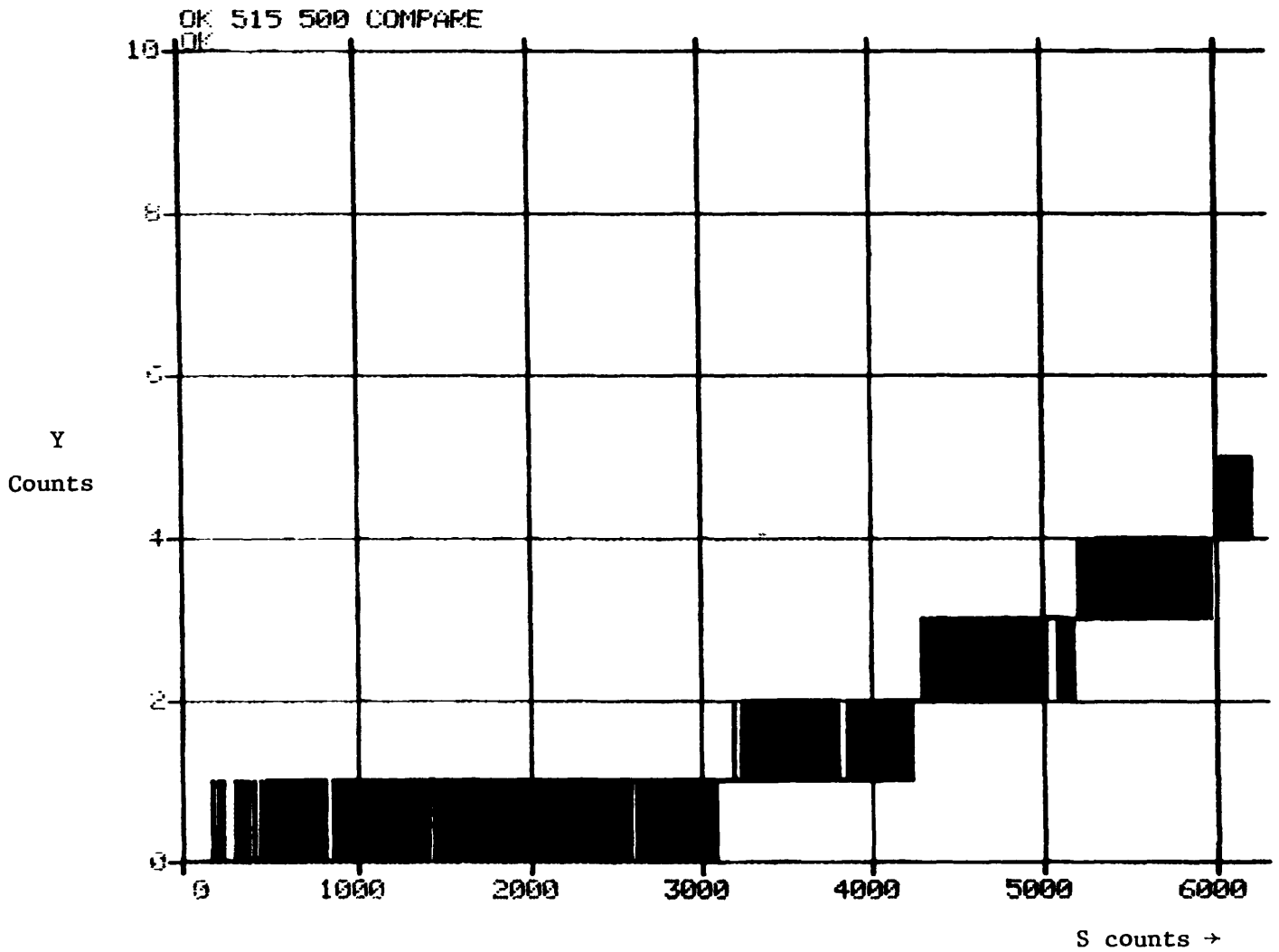


Figure 7 — The difference between the Y curves for two successive runs over the same radius of the dish. One Y count = 0.02 mm.

Figure 8 — (a) and (b) — Maps of the departures of the reflector surface from the best-fit paraboloid. (a) and (b) are derived from separate sets of measurements. Contour interval = 0.2 mm.

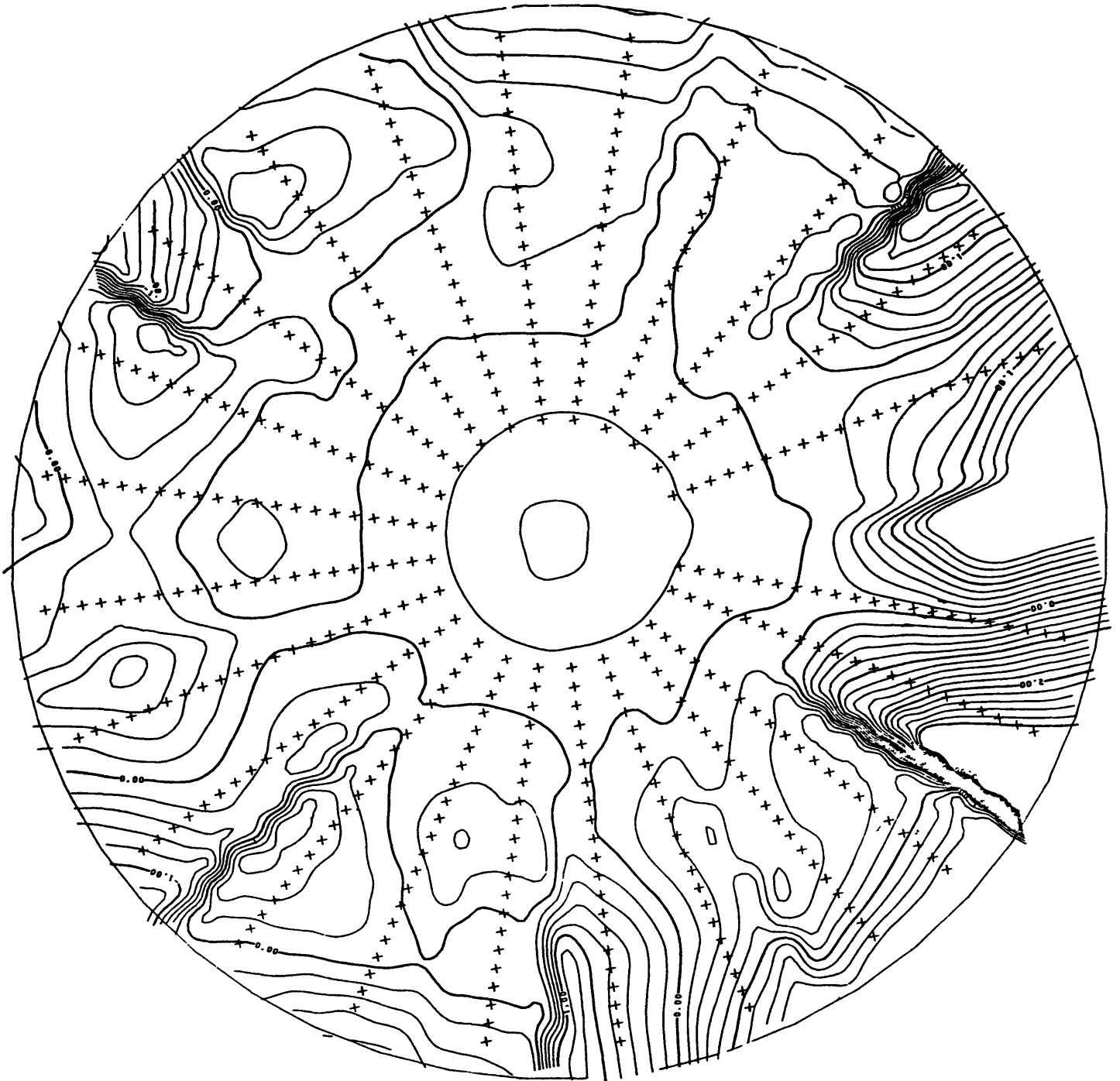


Figure 8(a)

Figure 8 - (a) and (b) - Maps of the departures of the reflector surface from the best-fit paraboloid. (a) and (b) are derived from separate sets of measurements.

Contour interval = 0.2 mm.

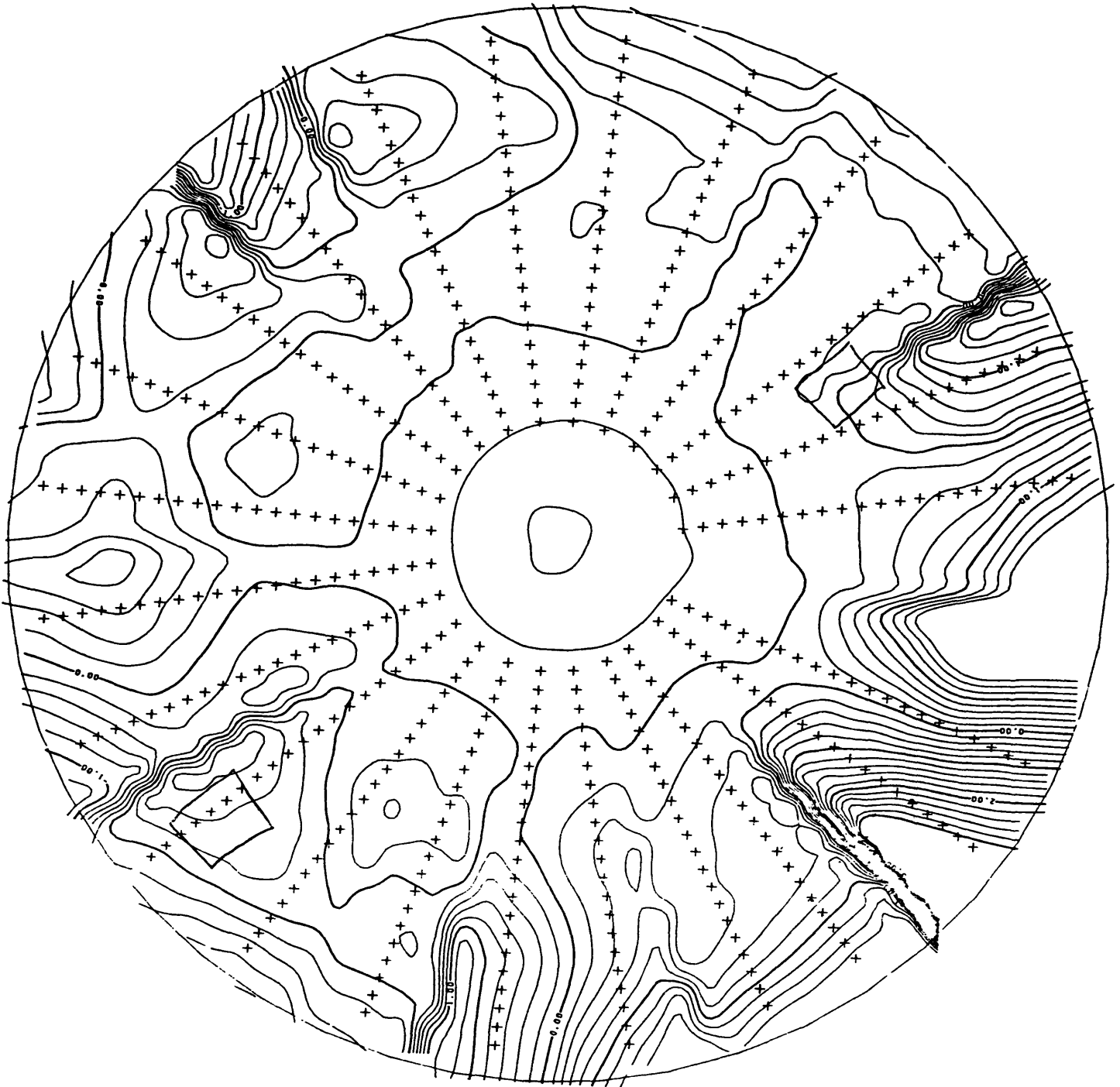


Figure 8(b)